

## STUDY OF WATER EFFECT ON THE PERFORMANCE OF A SPARK IGNITED ENGINE OPERATING WITH WET ETHANOL

**Rafael Lago Sari**, rafaellagosari@gmail.com

**Fernando Marcelo Pereira**, fernando@mecanica.ufrgs.br

Federal University of Rio Grande do Sul

Av. Paulo Gama, 110, Bairro Farroupilha, Porto Alegre, Rio Grande do Sul

CEP: 90040-060, Fone: 55 (51) 33086000

**Mario Eduardo Santos Martins**, mario@mecanica.ufsm.br

**Diego Golke**, diego\_golke@hotmail.com

Federal University of Santa Maria

Av. Roraima, nº 1000, Cidade Universitária, Bairro Camobi, Santa Maria - RS

CEP: 97105-900, 55 (55) 3220-7906

**Abstract.** Engine simulation is a very effective tool to reduce test bench time and to provide information that is difficult to measure directly in the internal combustion engines. Regarding combustion, detailed computational approaches are intrinsically complex due to its non-linear behavior. It often requires a thorough analysis in order to model phenomena like flame quenching and misfire leading to high computational cost. Thus, simplified phenomenological models incorporating mean flow characteristics and geometrical parameters are applied to achieve mean results. However, the lack of properties of some less ordinary fuels brings some difficulties on their application and may lead to mismatching results. The extensive use of hydrous ethanol and gasoline-ethanol blends in Brazil requires engine development to operate using them. Previous researches pointed out an increase in the ratio of energy spent/energy released using mixtures with hydration levels up to 20%. Hence, this work intends to validate a phenomenological turbulent combustion model for ethanol with water content of up to 30% (volumetric basis). A one-dimensional fluid dynamics computational model was built based on a port-fueled spark ignition engine. The pressure traces, fuel and air mass flows were acquired from the engine under test to be applied as boundary conditions for the combustion model in the 1-D simulation. Computational results were compared to experimental data showing good agreement for combustion parameters such as heat release rates and total combustion duration as well as main engine performance parameters, confirming the model's capability to simulate real test conditions.

**Keywords:** Internal combustion engines, turbulent combustion, numerical simulation.

### 1. INTRODUCTION

Alternative fuels have been proposed as substitutes for petroleum based fuels. Almost zero lifecycle CO<sub>2</sub> emission and semi perennial production of raw material justifies their use. Between these alternative fuels, ethanol plays a major role. It is considered one of the best fuels for internal combustion engines, showing elevated knock resistance, high burning speed and latent heat of evaporation as well as large flammability limits (Maclean & Lave, 2003). The use of ethanol-water mixtures with higher water content than conventionally used has received more attention in recent studies (Cordon, Beyerlein, Cherry, & Steciak, 2008; T. Lanzasova, DallaNora, & Zhao, 2016; Mack, Aceves, & Dibble, 2009; Martins, Lanzasova, & Sari, 2015). Although its use dates from 70's, it has been drawing attention for its low production cost and higher ratio between process energy input to fuel output when compared to the azeotrope ethanol. This occurs because in the production process the energy expenditure represents an exponential increase from 80% volumetric percentage of ethanol onwards. This greatly increases the final market price of ethanol (Michael R. Ladish, 1979).

A major review on the application of water addition in practical combustion system was carried out in (Dryer, 1977). It was stated that there would be small commercial interest with water addition due to transport costs implications. However, the water addition would promote an increase in knock resistance due to lower combustion temperatures. For this reason, some BMW vehicles use water injection in some high performance engines. In addition, the lower combustion temperatures leads to lower NO<sub>x</sub> emissions according to Zeldovich mechanism. It was also stated that the water addition in compression ignition engines as water-in-fuels emulsions would be an effective way to reduce diesel particulate emissions.

The use of ethanol-water mixtures with high water content, also called *wet ethanol*, in homogeneous charge compression ignition engines (HCCI), was extensively studied by Flowers et al. (Flowers, Aceves, & Frias, 2007), whose conducted a study using a turbocharged six-cylinder 2.4L caterpillar engine aiming to demonstrate that the use of wet ethanol in HCCI engines could improve the ethanol life cycle energy efficiency. For this, the peripheral systems were modelled using thermodynamic laws and the HCCI combustion was solved by an external CHEMKIM routine. Results demonstrated high engine conversion efficiency even for water percentages up to 35%, with low NO<sub>x</sub> emission levels and 14 % of overall energy saving. Saxena researched HCCI operation running with wet ethanol aiming to

determine the optimal engine operational conditions (Saxena et al., 2014; Saxena, Schneider, Aceves, & Dibble, 2012). The experimental tests were carried out in an four cylinder 1.9L TDI engine with compression ratio of 19,5:1. The HCCI operation was achieved by means of air heating with an exhaust heat recovery device. As results, a wide range of operation with wet ethanol was achieved.

The use of wet ethanol in spark ignition engines by (Munsin, Laoonual, Jugjai, & Imai, 2013) showed the implications of high water-in-ethanol percentage in performance and emissions of a small spark ignition engine for power generation. The results showed that mixtures containing up to 40% of water v/v could be used. Such fuels would be of especial interest in remote and rural areas where ethanol could be produced locally with simplified production methods. No tribological study was performed. Regarding emissions, the NO<sub>x</sub> emissions levels decreased dramatically as the water content increased. The impacts in performance and emissions were also evaluated by Martins et al. (Martins et al., 2015). For this, it was used a 0.668 L, single cylinder engine, containing a pre-chamber cylinder head. This is the same base engine used in the present study, but with a modified cylinder head. Stable operation could be achieved for water in-ethanol mixtures with up to 40% by volume. In addition, the increase in water content led to a direct decrease in NO<sub>x</sub> emissions. The same results were reported elsewhere (Ambrós et al., 2015).

Despite many works regarding wet ethanol application in internal combustion engines, the number of operating conditions addressed does not cover the full engine map. To contribute to this need, both numerical and experimental approaches are used in this work. Regarding the numerical approach, it is essential the modeling of the combustion process. A burning law must take into account effects of flow and geometric parameters of the engine in order to capture the main limiting phenomena of engine design and operation condition. Blizard and Kech were the first to propose a turbulent flame propagation model for ICE (Norman C. Blizard, 1974). Such model assumed that during the turbulent flame front propagation through the combustion chamber eddies having a characteristic radius  $l_e$  were entrained by the flame front at a turbulent entrainment velocity  $u_e$  burning at a characteristic time  $\tau = l_e/u_l$ . In addition, it was proposed an analytic method to determine the equilibrium state of the burned gases, which still extensively used in commercial 1D engine simulation codes. Correlations were developed to calculate both the entrainment speed  $u_e$  and the eddy radius  $l_e$  considering the engine geometry, fuel type and operating conditions.

Later, a turbulent entrainment model for turbulent premixed combustion process in SI ICE using the basic quantities of turbulent flow was proposed (Tabaczynski, Ferguson, & Radhakrishnan, 1977). The turbulent flow model was defined through the macro and micro scales of turbulence and turbulence intensity. The reaction time (the period that the entrained eddy takes to be burned) of large eddy was calculated based on the micro scale reaction time defined by the characteristic length divided by the laminar flame speed. The reaction time for the large eddies was related to the flame kernel development time and showed similar trends to ignition delay time. Comparisons with experimental data showed the model's capability to reproduce typical behavior of combustion duration with for distinct equivalence ratios, EGR fractions, spark time and engine speed.

A following work aimed to verify the previous model by means of a comparison of predicted ignition delay and combustion intervals with calculated values from experimental data (Hires, Tabaczynski, & Novak, 1979). Correlations based on fundamental flow quantities (turbulent integral scale, turbulent micro scale, turbulent intensity and laminar flame speed) were used. It was assumed that the turbulent integral scale was proportional to the instantaneous chamber height prior to the flame initiation while the turbulence intensity was related to the mean piston speed. Empirical constants were used to scale the correlations to a given engine. Several operating conditions were simulated and compared with experimental results.

A phenomenological SI combustion model was developed elsewhere (Syed Wahiduzzaman, Thomas Morel, 1993). It was based on turbulent flame concept linked to turbulence and in-cylinder flow calculation. The flame front behavior was modeled taking into account its interactions with the combustion chamber. The simulated traces were compared with experimental results to verify the model reliability. Generally, it was found good agreement between simulated and experimental results. Some difficulties were found at idle due to large cycle-by-cycle variability. Morel et al developed and combustion model that simulated the flame propagation as a spherically growing region originating at the spark location (T. Morel, C.I.Rackmil & Jennings, 1988). The instantaneous flame position was used as input directly into the heat transfer model and it was shown that the prediction of flame development has fundamental impact over the accurate heat transfer calculation. This way it was possible to determine heat transfer spatially across the combustion chamber. The rate of mass burned was assumed proportional to the flame front area and flame speed. The flame speed was calculated from a turbulence based entrainment model accounting for gas composition and the state of the mixture (pressure and temperature) on the laminar burnup behind the entrainment front. Heat flux and combustion durations predicted by the model were validated against experimental data.

Based on this, the present work intends to study the effect of the water-in-ethanol content on the performance of a port fuel injection single-cylinder spark ignition engine through experimental bench tests. The experimental pressure traces, fuel and air mass flow rates were used as inputs to a predictive model. The numerical tool was used to systematically explore the engine operational map, aiming at finding the optimum efficiency and lower emission conditions.

## 2. METODOLOGY

In this section, the experimental setup developed is described as well as the approaches applied to solve the in-cylinder flow and the combustion process. As a first step, a set of experimental data was collected (manifold and in cylinder pressure traces, fuel and air consumption, etc.) for some specific operational conditions. Afterwards, these experimental results were used as inputs and reference parameters to calibrate the computational model. In the last part of the present work, the calibrated model is explored to predict mean combustion parameters at intermediate conditions not covered by the experiments.

### 2.1 Experimental Setup

The bench tests were carried out in a single cylinder engine with the characteristics presented in table 1. Compression ratio was reduced to 13:1 to enable spark ignition combustion and to avoid knock while still offering good performance.

Table 1 Engine Characteristics

Parameter	Description
Number of cylinders	1
Bore x stroke (mm)	90.0 x 105.0
Displaced volume (cm <sup>3</sup> )	668
Compression ratio	13
Intake valve diameter (mm)	41.0
Exhaust valve diameter (mm)	35.0
Intake valve lift (mm)	9.0
Exhaust valve lift (mm)	9.5
Intake valve open	36° BTDC
Intake valve close	184° ATDC
Exhaust valve open	204° BTDC
Exhaust valve close	64° ATDC
Idle speed (rpm)	1200-1300

Table 2 sensors accuracy

Device	Accuracy
In-cylinder pressure transducer	0.3 % of Full Scale
Intake pressure transducer	1.5% of Full scale
Exhaust pressure transducer	1.5% of Full scale
Lambda meter	1.7% of measurements
Fuel flow	1.8% of measurements
Air Flow (calculated through lambda and fuel flow)	4.0 % of measurements
Load cell	0.03 of Output voltage
K type thermocouples	0.75% of measurements

The engine was instrumented with high frequency sensors in order to capture high frequency combustion phenomena. For intake and exhaust pressure measurements, two MPX 4250 AP piezo resistive sensors were installed. In-cylinder pressure measurements were performed with a piezoelectric AVL GH 14D. Thermocouples were installed to monitor exhaust and intake temperatures. Ambient air condition (humidity, temperature and pressure) were also monitored during the tests. Fuel consumption was measured on a volumetric basis using a 0.2 ml resolution burette, while the air consumption was calculated using fuel consumption and lambda values (measured with a Bosch 4.2 wide-band oxygen sensor). In each test, the engine was loaded with an eddy current dynamometer, which provided closed loop actuation for speed and torque (Roberto et al., 2016). A load cell was used in order to monitor the torque for each test condition and feed the dynamometer torque loop. National Instruments acquisition boards NI 6008 and NI 6250 were used to acquire all sensor signals. A LabVIEW routine allowed to monitor real time pressure traces and combustion parameters such as combustion duration, 50% of mass fraction burned (CA50), etc. Figure 1 presents the experimental setup. The tests were carried out keeping CA50 at 10 CAD after top dead center and constant engine load (BMEP=0.7 MPa) for water in ethanol mixtures of 7% 20% and 30% in volumetric content. Engine speed was kept in 1800 RPM due to Brazilian grid frequency for electric generation.

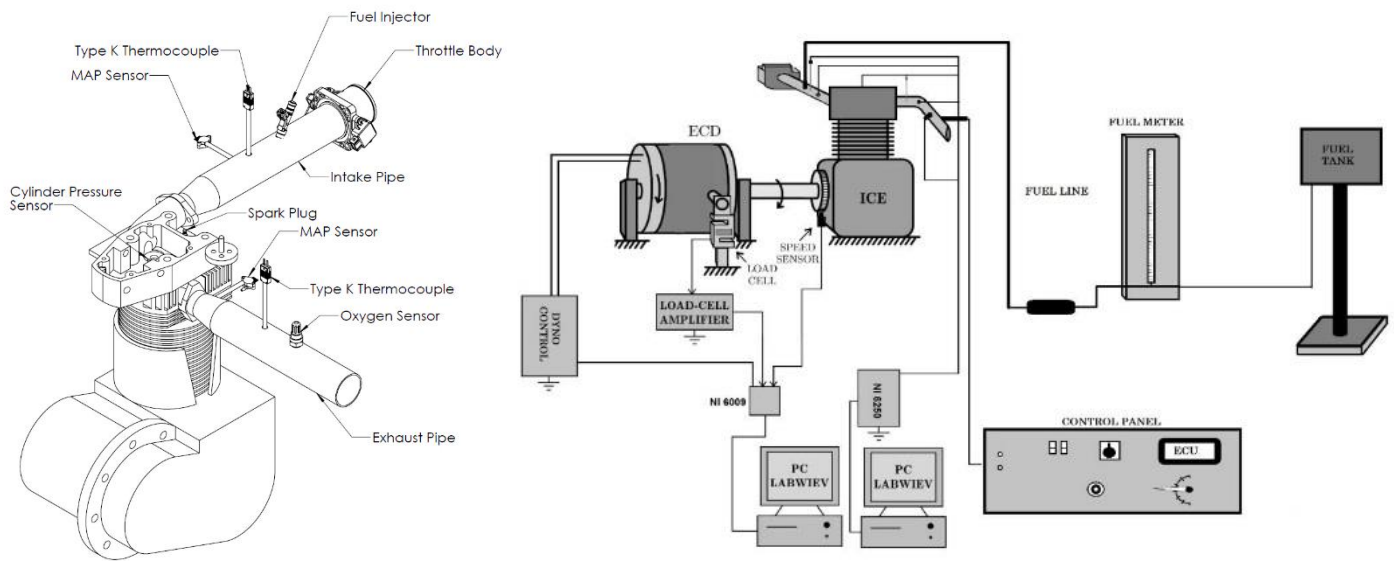


Figure 1 Experimental Setup and instrumentation

Each test was performed according to the following sequence:

- 1- Warm up phase
- 2- Load application.
- 3- Stabilization of lambda and ignition timing phasing to reach center of combustion in 10 CAD, ATDC.
- 4- Data acquisition and fuel consumption measurement
- 5- Recording of ambient condition.
- 6- New operation condition.

## 2.2 Numerical Modelling

Both heat release analysis and turbulence combustion calculation were performed in a commercial code, GT Power®, focused on engine R&D. It is an object-oriented package where each box represents an engine part where the related models can be chosen. Moreover, several auxiliary templates for monitoring and controlling engine parameters can be implemented. The model built is illustrated in Figure 2.

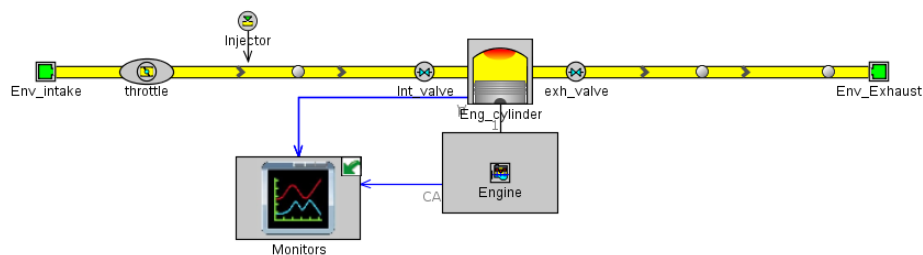


Figure 2 Gt Power model

### 2.2.1 Three Pressure Analysis (TPA) - Heat release calculation

This method uses in-cylinder pressure to determine the heat release rate, which is used in a two-zonal combustion model enabling calculations for the burned and unburned zones, instead of temperature-averaged parameters resulting from single-zone analysis. A modified Woschni model was used for heat transfer and the Chen-Flynn model was used for engine friction. Deeper explanation of the method and modeling theory used by GT-Power can be found in (Bos, 2007; GT-Power., 2015; T. D. M. Lanzanova, 2013). It is worth to state that this routine does not simulate the burning rate. Instead of this, it determine the burning rate from the experimental pressure traces through the first law of thermodynamics for a closed volume.

### 2.2.2 Predictive Combustion Flow and Combustion Approaches.

In GT-Power, the governing equations to solve in cylinder flow are located in EngCylFlow template. Its equations are fully described in Morel and Keribar work (T. Morel, C.I.Rackmil & Jennings, 1988). The combustion chamber is divided in three regions (squish area, cup volume and the region above the cup lip). Equations for turbulent kinetic energy,  $k$ , its dissipation rate,  $\epsilon$ , and angular momentum are solved in each of them. Regarding the modelling of turbulent combustion, it is performed through SI<sub>turbcomb</sub> template from GT-Power. Detailed description can be found on (T. Morel, C.I.Rackmil & Jennings, 1988). The governing equations are presented in 1-7. Equation 1 presents the total entrained mass rate of the unburned gas. It can be seen that this rate is proportional to the flame area, the unburned gas density and an entrainment velocity given by the sum of the laminar and the turbulent flame speeds.

$$\frac{dM_e}{dt} = \rho_u A_e (S_T + S_L) \quad (1)$$

where,

$M_e$  : entrained mass

$\rho_u$  : unburned gas density

$A_e$  : Effective flame front area

$S_T$  : turbulent burning velocity

$S_L$  : laminar burning velocity

The laminar flame speed correlation is presented in equation 2. The software presents a database for ordinary fuels, such as gasoline, anhydrous ethanol. In this work, the values of anhydrous ethanol properties were assumed to be used as inputs for simulation.

$$S_L = (B_m + B_\Phi (\Phi - \Phi_m)^2) \left( \frac{T_u}{T_{ref}} \right)^\alpha \left( \frac{P}{P_{ref}} \right)^\beta f(Dilution) \quad (2)$$

Where,

$B_\Phi$  : laminar speed roll-off value

$B_m$  : maximum laminar speed

$f(Dilution) = 1.0 - 0.75 \cdot DEM \cdot (1.0 - (1.0 - 0.75 \cdot DEM \cdot Dilution)^7)$

$DEM$  : dilution effect multiplier

$Dilution$  : mass fraction of residuals in the unburned zone

$\alpha$  : temperature exponent

$\beta$  : pressure exponent

The effect of the in-cylinder turbulent flow in combustion is taken into account in the determination of turbulent flame speed values where the turbulence intensity calculated in the flow model is applied to find the  $S_T$  value.

$$S_T = C_s u' \left( 1 - \frac{1}{1 + \frac{C_k R_f^2}{L_t^2}} \right) \quad (4)$$

Where,

$C_k$  : Flame kernel Growth Multiplier

$R_f$  : flame radius

$L_t$  : turbulent length scale

$C_s$  : turbulent flame speed multiplier

$u'$  : turbulence intensity

The burnup process behind the flame front is assumed proportional to the entrained unburned mass behind the flame front. Hence, the equation for the burned mass rate is stated as:

$$\frac{dM_b}{dt} = \frac{M_e - M_b}{\tau} \quad (5)$$

Where,

$\tau$  = time constant given by:

$$\tau = \frac{\lambda}{S_L} \quad (6)$$

And  $\lambda$ , the Taylor scale:

$$\lambda = \frac{C_\lambda L_t}{\sqrt{R_{e_t}}} \quad (7)$$

Where,

$C_\lambda$  : Taylor length scale Multiplier

$R_{e_t}$  : turbulent Reynolds

The constants  $C_s$ ,  $C_k$ ,  $L_t$  and DEM are found via an optimizer algorithm, which targets the minimum RMS error between the simulated and experimental pressure traces. For this, it is used at least 22 real operation conditions in order to find only one set of constant values. All fuel properties used were assumed the same as for anhydrous ethanol.

### 3. RESULTS

#### 3.1 Heat release Analysis

This section presents the results found through experiments and heat release analysis (TPA). The burned fuel fraction curves FFTM (fraction of total fuel mass) demonstrate the decrease in the burn rate as the water percentage increases. This can be visualized comparing the curves slope in Figure 3 a. The water concentration has a direct impact on the mixture transport properties increasing heat capacity values. Consequently, the temperature levels reached in combustion are lower than to those obtained for anhydrous ethanol leading to lower flame velocities whilst decreasing the slope in mass fraction burned curves. In order to maintain the CA50 in 10 CAD after TDC, the spark time was advanced. Hence, the longer time to burn the more hydrated mixtures was balanced by an early ignition. This is shown in Figure 3 b. The heat release profiles indicate an early energy release for E80W20 and E70W30 mixtures compared to E93W7 (standard ethanol fuel). This is attributed to the more advanced spark times for these mixtures. However, there is a decrease in the peak of heat release in the top dead center vicinity resulting in lower thermodynamic efficiencies, since in the ideal cycle all energy is released in a constant volume and adiabatic process.

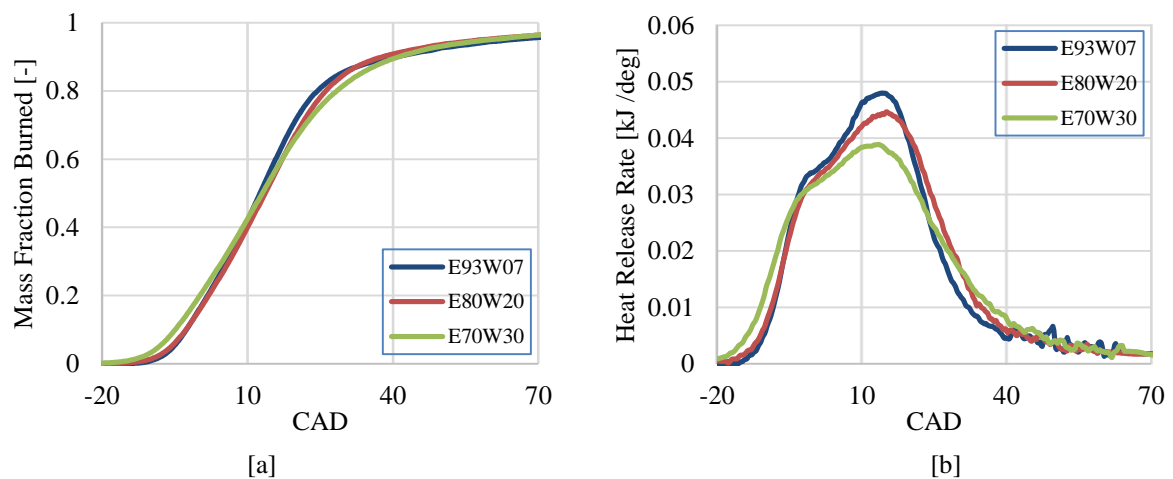


Figure 3: (a) burned fuel fraction for several water percentages, (b) heat release rate for several water percentages.

The ignition delay traces, defined as the time to burn 2% of the fresh charge related to the spark discharge, showed that high water concentration affects directly the initial flame development. This first phase is related to flow motion, pressure and temperature conditions as well as the mixture composition. As the concentration of water increases, more energy is required to maintain the combustion process. This behavior is illustrated in Figure 4 a. Which regards brake efficiency, it is possible to see its decrease previously stated. As mentioned above, the heat release profiles showed higher deviation from ideal cycle as water percentage increases leading to lower thermodynamic efficiencies. The effect on engine brake efficiency is presented in Figure 4 a.

The assumption that the combustion of highly hydrated mixtures results in lower temperatures is sustained by Figure 4 b. These values were obtained from the heat release analysis based on the two-zone combustion approach. Hence, it is also possible to state that the heat diffusion from burned zone to unburned zone will decrease resulting in lower unburned zone temperatures. This effect reduces the knock occurrence probability allowing exploring higher compression ratios. Figure 4 b shows the covariance of indicated mean effective pressure. This parameter indicates the cycle-to-cycle combustion variability where  $COV_{IMEP}$  values of up to 5% indicate low combustion variability. It is possible to verify that stable operation was achieved for all mixtures.

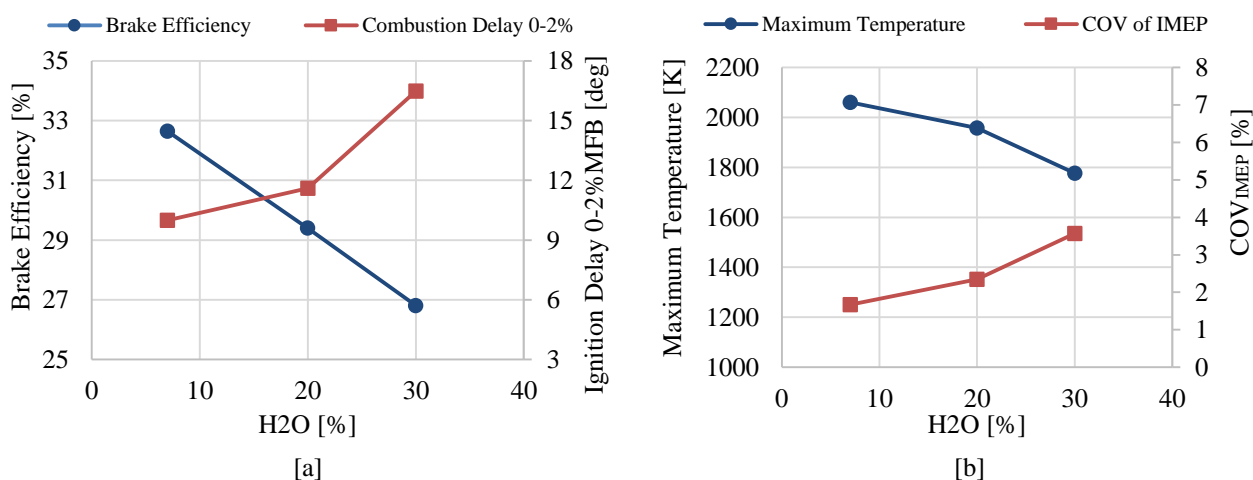


Figure 4: (a) brake efficiency values and combustion delay for several water percentages, (b) Maximum cycle temperature and  $COV_{IMEP}$  values versus hydration levels.

### 3.2 Predictive combustion results

Due to the change in fuel properties with water percentage, the optimization procedure available in GT-Power was not able to find only one set of constants values. The parameters related to the dilution effect and kernel development did not converged. This model deficiency requires a full description of laminar flame velocities; pressure and temperature exponents for each fuel blend instead standard ethanol properties. This will be addressed in future works. In this paper, the local solution for each blend was used for these two parameters.

The results using the predictive combustion model were compared to experimental and TPA results in order to check its capability to solve engine combustion. As it can be seen in figure 5, there is a good agreement between the simulated and TPA pressure traces. Hence, the heat release profiles for the most hydrated blend (E70W30) were compared and presented in Figure 5 [b]. The noisy trace results from the non-filtered experimental pressure trace. It can be concluded that the model can predict with good agreement the combustion heat release, since the maximum values obtained for both and its behavior are very similar. It is also possible to check that the model does not fit exactly the heat release profile near of the TDC point. The change in curve slope in the experimental trace was approximated by average values for this point. The impact of this behavior must be investigated since large differences are expected for different and complex combustion chamber geometries.

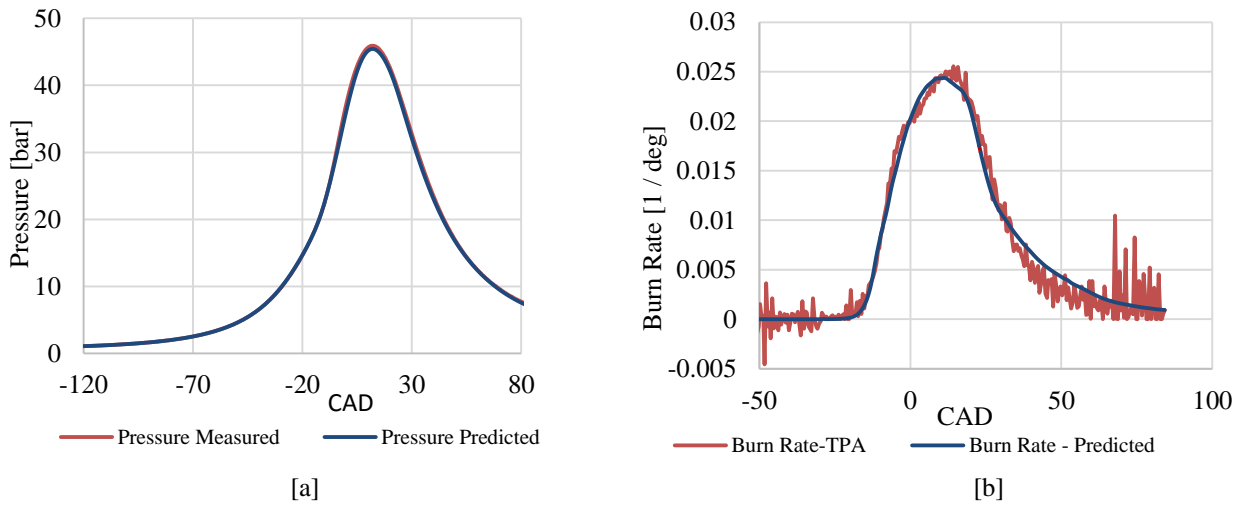


Figure 5: (a) pressure comparison for experimental, TPA and simulated results, (b) burn rate comparison for simulated and TPA results.

As a final verification, the crank angle related energy balance was analyzed as presented by Figure 6 a. It takes into account variations in internal energy, heat transfer and work during combustion and the beginning of the expansion stroke. The comparison between TPA and simulated results for these three properties presented similar values. Since the heat transfer model is the same for both cases, it is also possible to verify that the instantaneous pressure and temperature values are closer than to the experimental ones. Based on this, the same operation conditions presented in the previous section were simulated with the calibrated model and the combustion parameters were compared. The results are presented in Figure 6 b. It can be verified that the values obtained for combustion duration (10-90% MFB) and the combustion delay are closer to those obtained from TPA results. However, there are differences mainly for the E93W7 fuel since the two model constants were averaged, favoring the more hydrated mixtures.

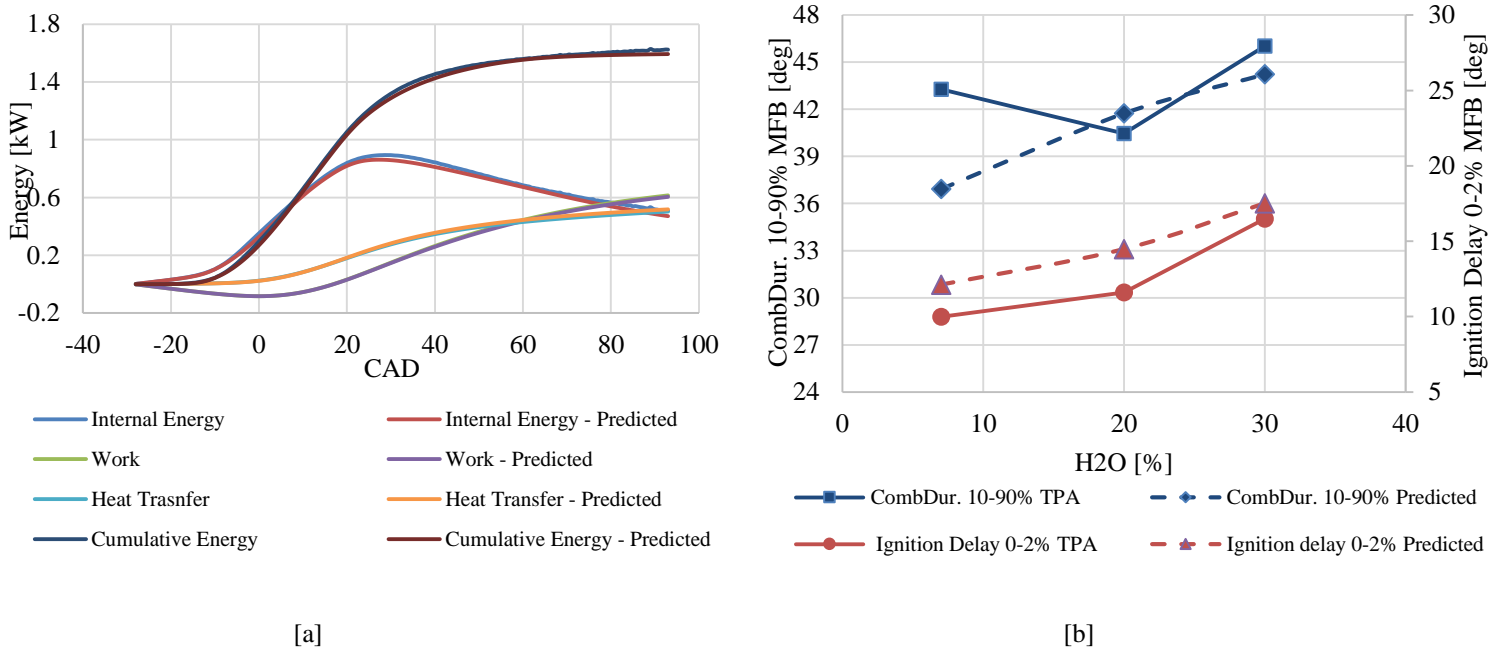


Figure 6: (a) experimental and simulated in-cylinder balance comparison for E70W30, (b) comparison of the values of ignition delay and combustion duration 10-90% MFB obtained by TPA and predictive combustion model.

#### 4. CONCLUSIONS

The present work demonstrated the effects of using highly hydrated mixtures of ethanol and water on the performance and combustion parameters of a spark-ignited engine. As conclusion, it was found stable operation for all mixtures, with COVIMEP smaller than 5%. However, parameters such as brake efficiency and ignition delay highlighted the negative effect of water increase in combustion process. The heat release profiles demonstrated slower combustion as the water content increases. In addition, the lower in-cylinder maximum temperatures indicate that it is possible to apply high compression ratio or boosted operation in order to improve the cycle efficiency.

A predictive combustion model from GT-Power was also calibrated. The results indicated good agreement between simulated and experimental traces. However, several model deficiencies were detected. The model does not take into account the water effect on laminar flame velocities and flame development. Therefore, it is not possible to decouple the optimization and water percentages. In addition, it does not incorporate the effect of complex combustion chamber geometries on heat release profiles. Then, it is necessary a detailed combustion investigation to determine combustion properties as the pressure and temperature exponent in laminar flame velocity equation for high hydrated mixtures. This will be addressed in future works.

#### 5. ACRONYMS LIST

Acronyms	Definition
ATDC	<i>After Top Dead Center</i>
BMEP	<i>Brake Mean Effective Pressure</i>
BTDC	<i>Before Top Dear Center</i>
CA50	<i>Crank angle of 50&amp; of mass fraction burned</i>
CAD	<i>Crank Angle Degree</i>
COV	<i>Covariance</i>
FFTM	<i>Fraction of Fuel Total Mass</i>
ICE	<i>Internal Combustion Engine</i>
IMEP	<i>Indicated Mean Effective Pressure</i>
MFB	<i>Mass Fraction Burned</i>
SI	<i>Spark Ignition</i>
TDC	<i>Top Dead Center</i>
TPA	<i>Three Pressure Analysis</i>

#### 6. REFERENCES

- Ambrós, W. M., LanzaNova, T. D. M., Fagundes, J. L. S., Sari, R. L., Pinheiro, D. K., Martins, M. E. S., & Salau, N. P. G. (2015). Experimental analysis and modeling of internal combustion engine operating with wet ethanol. *Fuel*, 158, 270–278. <http://doi.org/10.1016/j.fuel.2015.05.009>
- Bos, M. (2007). Validation Gt-Power Model Cyclops Heavy Duty Diesel Engine, pp. 1 – 110.
- Cordon, D., Beyerlein, S., Cherry, M., & Steciak, J. (2008). HOMogeneous Charge Catalytic Ignition of Ethanol-Water/Air Mixtures in a Reciprocating Engine., 1–10.
- Dryer, F. L. (1977). *Water addition to practical combustion Systems - Concepts and applications*.
- Flowers, D. L., Aceves, S. M., & Frias, J. M. (2007). Improving Ethanol Life Cycle Energy Efficiency by Direct Utilization of Wet Ethanol in HCCI Engines, 1070–1078.
- GT-Power. (2015). Engine Performance.
- Hires, S. D., Tabaczynski, R. J., & Novak, J. M. (1979). The Prediction of Ignition Delay and Combustion Intervals for a Homogeneous Charge , Spark Ignition Engine. *SAE Technical Paper 780232*, 1053–1067. <http://doi.org/10.4271/780232>
- LanzaNova, T. D. M. (2013). *Avaliação Numéirica e Experimental do desempenho de um motor Otto Operando com etanol hidratado*. Federal Unirsity of Rio Grande do Sul.
- LanzaNova, T., DallaNora, M., & Zhao, H. (2016). Performance and economic analysis of a direct injection spark ignition engine fueled with wet ethanol. *Applied Energy*, 169, 230–239. <http://doi.org/10.1016/j.apenergy.2016.02.016>
- Mack, J. H., Aceves, S. M., & Dibble, R. W. (2009). Demonstrating direct use of wet ethanol in a homogeneous charge compression ignition (HCCI) engine. *Energy*, 34(6), 782–787. <http://doi.org/10.1016/j.energy.2009.02.010>
- Maclean, H. L., & Lave, L. B. (2003). Evaluating automobile fuel / propulsion system technologies, 29, 1–69.
- Martins, M., LanzaNova, T., & Sari, R. (2015). Low Cost Wet Ethanol for Spark-Ignited Engines : Further Investigations. *SAE Technical Paper*. <http://doi.org/10.4271/2015-01-0954>
- Michael R. Ladish, K. D. (1979). Dehydration of ethanol-new approach gives positive energy balance. *Science*.

- Munsin, R., Laoonual, Y., Jugjai, S., & Imai, Y. (2013). An experimental study on performance and emissions of a small SI engine generator set fuelled by hydrous ethanol with high water contents up to 40%. *Fuel*, *106*, 586–592. <http://doi.org/10.1016/j.fuel.2012.12.079>
- Norman C. Blizard, J. C. K. (1974). Experimental and Theoretical Investigation of Turbulent Burning Models for Internal Combustion Engines. *SAE Technical Paper Series*.
- Roberto, J., Rafael, T., Sari, L., Diórdinis, T., Lanzasova, M., Eduardo, M., ... Pinheiro, H. (2016). Modeling and Control of a Low-Cost Driver For an Eddy Current Dynamometer. *Journal of Control, Automation and Electrical Systems*, (Imd). <http://doi.org/10.1007/s40313-016-0244-4>
- Saxena, S., Schneider, S., Aceves, S., & Dibble, R. (2012). Wet ethanol in HCCI engines with exhaust heat recovery to improve the energy balance of ethanol fuels. *Applied Energy*, *98*, 448–457. <http://doi.org/10.1016/j.apenergy.2012.04.007>
- Saxena, S., Vuilleumier, D., Kozarac, D., Kriek, M., Dibble, R., & Aceves, S. (2014). Optimal operating conditions for wet ethanol in a HCCI engine using exhaust gas heat recovery. *Applied Energy*, *116*, 269–277. <http://doi.org/10.1016/j.apenergy.2013.11.033>
- Syed Wahiduzzaman, Thomas Morel, S. S. (1993). Comparison of Measured and Predicted Combustion Characteristics of a four-valve S.I. Engine. *SAE Technical Paper Series*.
- T. Morel, C.I.Rackmil, R. K., & Jennings, M. J. (1988). Model for Heat Transfer and Combustion in Spark Ignited Engines and Its Comparison with Experiments. *SAE Technical Paper Series*.
- Tabaczynski, R. J., Ferguson, C. R., & Radhakrishnan, K. (1977). A Turbulent Entrainment Model for Spark-Ignition Engine Combustion. *SAE Technical Paper Series*, (770647), 2414–2433. <http://doi.org/10.4271/770647>

## 7. RESPONSIBILITY NOTICE

The authors are the only responsible for the printed material included in this paper.